Fuel 347 (2023) 128438

Contents lists available at ScienceDirect

Fuel

journal homepage: www.elsevier.com/locate/fuel

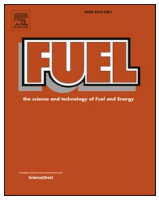

Full Length Article

New biodegradation degree proxies based on acids and neutral nitrogen- and oxygen-containing compounds characterized by high resolution mass spectrometry

Dongyong Wang [a], Meijun Li [b,*], Dingsheng Cheng [c,*], Yebo Du [c], Quan Shi [d], Xianli Zou [b], Qingyao Chen [e]

[a] State Key Laboratory of Petroleum Resources and Prospecting, China University of Petroleum (Beijing), Beijing 102249, China
[b] Faculty of Petroleum, China University of Petroleum-Beijing at Karamay, Karamay 834000, China
[c] Research Institute of Petroleum Exploration and Development, PetroChina, Beijing 100083, China
[d] State Key Laboratory of Heavy Oil Processing, China University of Petroleum, Beijing 102249, China
[e] Exploration and Development Research Institute, Jiangsu Oilfield Company, SINOPEC, Yangzhou, Jiangsu 225009, China

ARTICLE INFO

Keywords:
ESI FT-ICR MS
Biodegradation
Petroleum acids
Polar NSO compounds
Bongor Basin

ABSTRACT

Heavy oil is one of the most significant unconventional petroleum resources and one of its formation mechanisms is biodegradation. The characterization of the molecular compositions of petroleum is crucial for determining the various degrees of biodegradation. In this work, detailed investigations of acids and polar NSO compounds in different levels of biodegraded oils from the Bongor Basin (Chad) were carried out by negative ion electrospray ionization (-ESI) Fourier transform ion cyclotron resonance mass spectrometry (FT-ICR MS). The present findings show that the heteroatomic compounds of biodegraded crude oils are predominantly composed of N_1, N_1O_1, O_1, O_2, O_3 and O_4 species. The relative content of N_1, N_1O_1 and O_1 species tend to decrease and those of O_2, O_3 and O_4 species appear to increase with the increasing of biodegradation. The ratio of acyclic and cyclic acids (A/C ratio) of the O_2 species increase with an increase of biodegradation, indicating the increasing of O_2 class during microbial alteration. A new parameter, i.e. the ratio of $(O_2 + O_3 + O_4)/(N_1 + O_1)$ species, is presented to quantificationally define biodegradation levels. This parameter is inversely proportional to API gravity and has a favorable positive correlation with total acid number (TAN), suggesting acidic compounds are formed by the microbial alteration of N_1 and O_1 class and are more presented in advanced biodegradation. A modified ternary diagram including N_1, O_1 and $O_2 + O_3 + O_4$ species describe the detailed changes of nitrogen- and oxygen-containing compounds. Data points with a high level of biodegradation tend to shift to $O_2 + O_3 + O_4$ species end-member and retreat from N_1 species end-member, showing the relative content of $O_2 + O_3 + O_4$ species increase and those of N_1 species decrease with increasing biodegradation which may due to the formation of organic acids in degradation oil. The ratio of $(O_2 + O_3 + O_4)/(N_1 + O_1)$ species and the modified ternary diagram provide new parameters to estimate the biodegradation degree and TAN in crude oil.

1. Introduction

With the sharp growth of energy demand and the rapid decrease of conventional resources, unconventional resources including heavy oil attract more and more attention [1–3]. Biodegradation is a common and important process in the formation of subsurface heavy oil reservoirs, particularly in the context of late basin uplifting [4–6]. The reservoir temperature dropped and is now suitable for microorganism survival [7]. During biodegradation, normal alkanes in crude oil are first consumed by microorganisms, followed by branched alkanes, naphthenes (monocyclic and polycyclic), diasteranes and aromatic steroids [8–14]. Consequently, based on the sequence of selectivity in preferential removal compounds, the biodegradation index has been proposed to determine the grade of biodegradation [15,16]. A decrease of saturated and aromatic hydrocarbon fractions in crude oil resulting in a decrease in oil API gravity and an increase in total acid number (TAN) [17]. Thus, the heteroatomic compounds i.e. nitrogen-, sulfur- and oxygen-containing compounds, are predominate in biodegraded oil and

* Corresponding authors.
E-mail addresses: meijunli@cup.edu.cn (M. Li), chengdingsheng@petrochina.com.cn (D. Cheng).

https://doi.org/10.1016/j.fuel.2023.128438
Received 20 February 2023; Received in revised form 30 March 2023; Accepted 14 April 2023

could provide significant information to understand the related oil accumulation history. However, the heteroatomic compounds are characterized by a strong polarity and high boiling point, which makes those compounds difficult to separate and enrich. The conventional mass spectrograph, such as gas chromatographic-mass spectrometry (GC–MS) and gas chromatographic-mass spectrometry/mass spectrometry (GC–MS/MS), are inherently low resolution and poor ionization performance, leading to difficulty to represent the distribution of non-hydrocarbon constituents.

In recent years, Fourier transform ion cyclotron resonance mass spectrometry (FT ICR MS) is introduced into the field of petroleum geology and is considered as a useful tool to investigate polar NSO compounds [18]. This technology enables to direct measure basic and sulfur-containing compounds in positive ion electrospray ionization mode (+ESI) and acids and natural polar compounds in negative ion electrospray ionization mode (-ESI) [19]. Its resolving power and accuracy can be hundreds of thousands or even millions of times in the relative molecular mass range of the petroleum components (200–1000 Da) as high as GC–MS and GC–MS/MS. The polar compounds of petroleum can be completely separated and the number of atoms of C, H, O, N, and S elements can be calculated in different compounds using FT ICR MS. Hence, it has been applied for molecular composition measurement of petroleum [20–23], oil-source correlation [24–29], maturity definition [30–36], petroleum secondary migration [37,38], biodegradation process of petroleum [39–44] and origins of high acid oil [45–54]. For example, Kim et al. (2005) reported the change of acids and polar NSO compounds during secondary alteration of petroleum and proposed a new parameter i.e. A/C ratio (Acyclic/Cycle acids ratio), to quantificationally determine the degree of biodegradation of crude oil [55]. Li et al. (2010) hold that biodegradation is an important factor for the origin of high acidity crude oil [47].

In this paper, eight crude oils with different levels of biodegradation were investigated by (-) ESI FT ICR MS. Meanwhile, the distribution of oxygen- and nitrogen- containing compounds was systematically observed and analyzed due to microbial alteration.

2. Geological setting

The Bongor Basin, located in Central African Shear Zone (CASZ), is a Mesozoic–Cenozoic continental rift basin resulted from the Central Africa dextral strike-slip fault [56,57] (Fig. 1a). The Bongor Basin, covers an area of 1.8×10^4 km^2, is a significant petroliferous basin in Chad [58]. It was divided into four secondary structural units: southern depression, southern uplift, central depression and northern slope from south to north (Fig. 1b). Major discovered oil accumulations occurred in the northern slope, including Baobab oilfield, Mimosa oilfield, Ronier oilfield and Prosopis oilfield [59,60]. The intensive structural movement in the late Cretaceous caused inversion structural styles in the basin. The study area is characterized by predominantly NW-SE trending faults [61,62] (Fig. 1b).

In the study area, the Prosopis Formation and Mimosa Formation in Lower Cretaceous are considered as main source beds (Fig. 1c). The source rocks bear a high abundance of organic matter (average total organic carbon > 3.5%) and are characterized by type II kerogen. Oil accumulations occurred in the various strata in Cretaceous [59] (Fig. 1c). The discovered oils in northern slope are comparable in organic geochemistry and are classified as an oil family. Those oils are characterized by high wax content (average 22.3%), low sulfur contents (average 0.12%) [63,64].

3. Samples and experiments

3.1. Samples

Eight crude oil samples were collected from seven wells in the northern slope in this basin (Table 1), two wells in the Ronier oilfield,

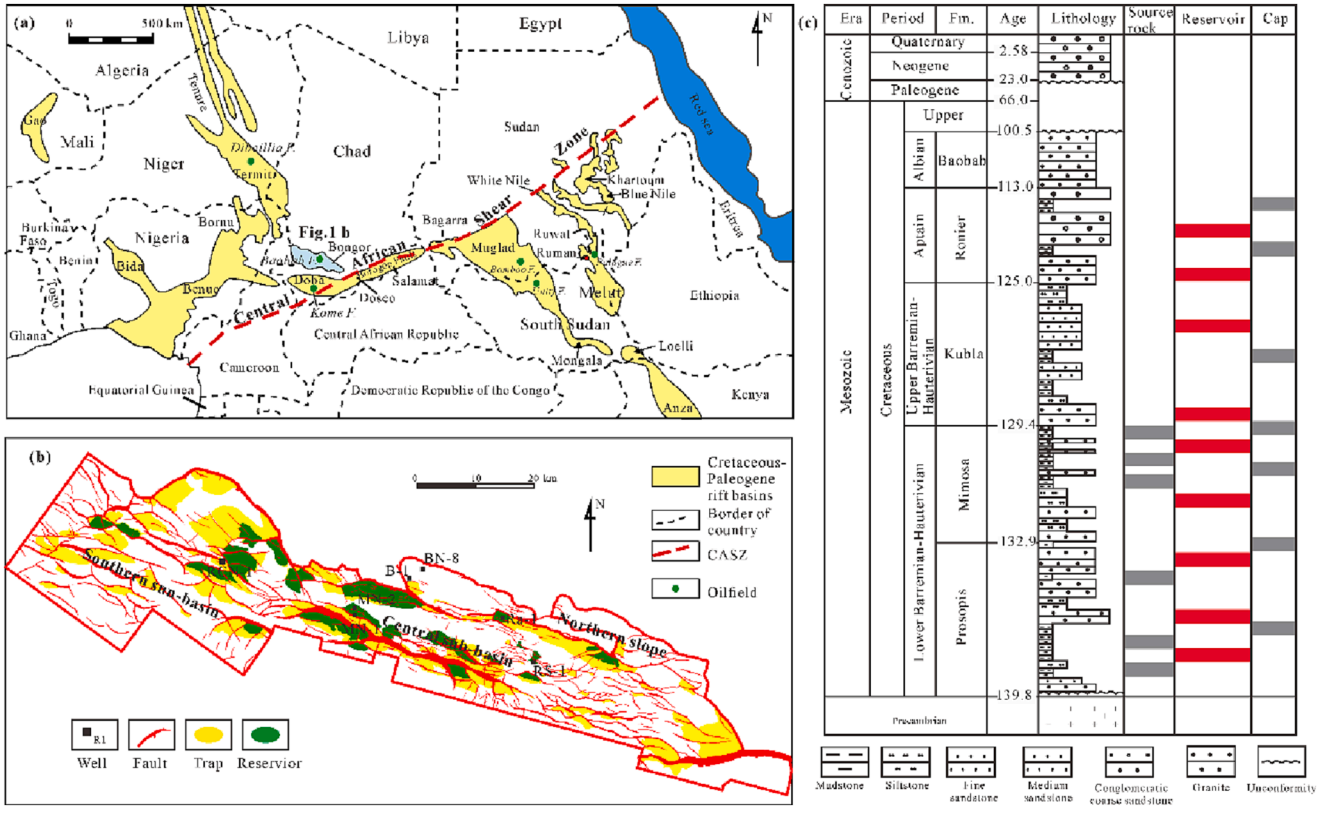

Fig. 1. (a) Location of Central African Shear Zone (CASZ) and Bongor Basin; (b) distribution of faults, reservoirs and traps in the Bongor Basin and sampled wells in the area; (c) comprehensive stratigraphic profile of the Cretaceous strata in the study.

Table 1
Physical and geochemical properties of crude oil samples from Bongor Basin, CASZ.

PM	Well	Depth (m)	Fm.	Sat (%)	Aro (%)	NSO (%)	Asp (%)	API (°)	TAN mg/g
0	RS-1	980.86–990.46	K	61.46	14.97	14.24	9.34	34.19	nd
1	R-1	1051.00–1053.00	K	67.45	13.85	14.44	4.26	29.28	0.05
2	BN-8	1388.00–1407.70	P	59.37	15.98	20.45	4.19	28.33	0.15
3	MN-2	896.70–976.20	K	19.53	54.78	20.70	5.00	21.08	1.42
4	MN-1	866.00–873.00	K	56.11	23.15	12.41	8.33	28.50	1.09
5	R-1	526.00–532.00	K	43.81	24.03	20.15	12.01	15.44	0.14
6	B-1	542.00–554.00	K	44.55	22.27	17.73	15.45	16.87	3.21
7	RCN-1	1014.40–1024.00	R	50.94	24.23	16.29	8.54	12.89	8.12

Notes: PM: Biodegradation index based on [15]; Fm: Formation, K-Kubla, P-Prosopis; Sat: the content of saturated hydrocarbons in oil, wt%; Aro: the content of aromatic hydrocarbons in oil, wt%; NSO: the content of gelatine in oil, wt%; Asp: the content of asphaltenes in oil, wt%; API: gravity, °; TAN: total acid number, mg KOH/g oil; nd: no data.

one well in the Prosepis oilfield, two wells in the Baobab oilfield and one well in the Raphia oilfield (Fig. 1b). Cheng et al. (2022) proposed that those oils have similar maturity, common origins and are likely to belong to the same oil group [63].

3.2. Gas chromatography (GC)

The Gas chromatography were carried out in an Agilent 7890A equipment with a HI-1 elastic capillary column (60 m × 0.25 mm × 0.25 μm). The initial temperature was 40 ℃ for holding 10 min, and then programmed to 70 ℃ at a rate of 4 ℃/min, and finally to 300 ℃ at a rate of 8 ℃/min for holding 40 min. The carrier gas was helium (purity > 99.999%) and its flow rate was 1 mL/min.

3.3. Gas chromatography-mass spectrum (GC–MS)

GC–MS analyses of the saturated fractions were carried out on a 5975A instrument, equipped with an HP-5MS chromatographic column (30 m length, 0.25 mm inner diameter, and 0.25 μm film thickness). Helium (purity > 99.999%) was used as the carrier gas. The oven temperature was initially set at 50 ℃, with one-minute hold. It was then raised to 120 ℃ at 20 ℃/min during the first stage, and then to 310 ℃ at 3 ℃/min during the second stage, where it was held for 20 mins. Electron impact ionization (70 eV) was employed.

3.4. (-) ESI FT ICR MS

The crude oil analyzed by negative ion (-) ESI FT-ICR MS by a Bruker Apex-Ultra mass spectrometer equipped with a 9.4 T superconducting magnet to measure the polar and acid (Nitrogen- and oxygen-containing) compounds. The oil sample was injected to ESI source at a rate of 250 μL/h. The spray voltage is −4000 V, and the front voltage and the end voltage of capillary column are −4500 V and 320 V, respectively. The mass range was set from *m/z* 100 to 1000. The detailed FT-ICR-MS mass calibration and data analysis methods are described by Shi et al. (2010) [22].

4. Results

4.1. Degree of biodegradation of crude oils

The inversion tectonic movement resulted in the strong erosion of the Upper Cretaceous and oils had been biodegraded in different levels. The molecule markers in non-degraded oil (PM = 0) are complete (Fig. 2a, Fig. 3a). Samples of PM = 1, 2 and 3 occur obvious loss of *n*-alkanes (Fig. 2 b; Fig S1 b–d). Sample of PM = 4 exhibits a complete depletion of *n*-alkanes and isoprenoid (Fig S1 e). However, it is no distinct difference for the distributions of saturated biomarkers in samples of from PM = 0 to PM = 4 (Fig. 3a). The relative abundance of tricyclic terpenes is significantly enhanced in samples of PM = 5 (Fig S2b). Sample of PM = 6 occurs 25-norhopanes [65] and discernable hopane distributions (Fig S2 c). Sample of PM = 7 is characterized by high content of 25-norhopanes but less of tricyclic terpenes and hopanes (Fig. 2b).

4.2. Compound class distribution

The selected oil samples are characterized by high abundance of N- and O- containing compounds. In the non-degraded oil, N_1 compounds are the dominated species, followed by O_2, O_1, N_1O_1 and N_1O_2 classes (Fig. 4) (Table S1). The relative abundance of sulfur-containing compounds is much lower than N- and O- containing compounds.

Biodegradation in various degrees obviously affected the distribution of compound classes. Overall, the relative content of N_1, N_2, N_1O_1, N_1O_2

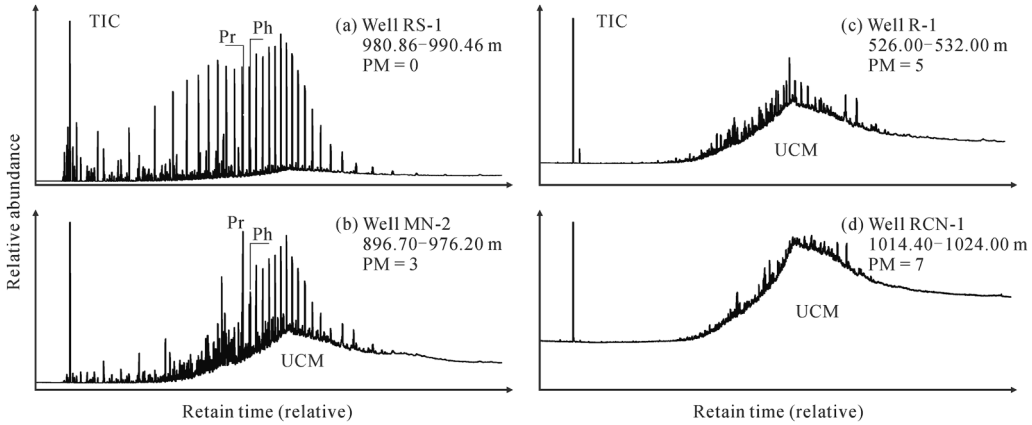

Fig. 2. Representative total ion currents (TICs) of different levels of biodegradation crude oils from the Bongor Basin.

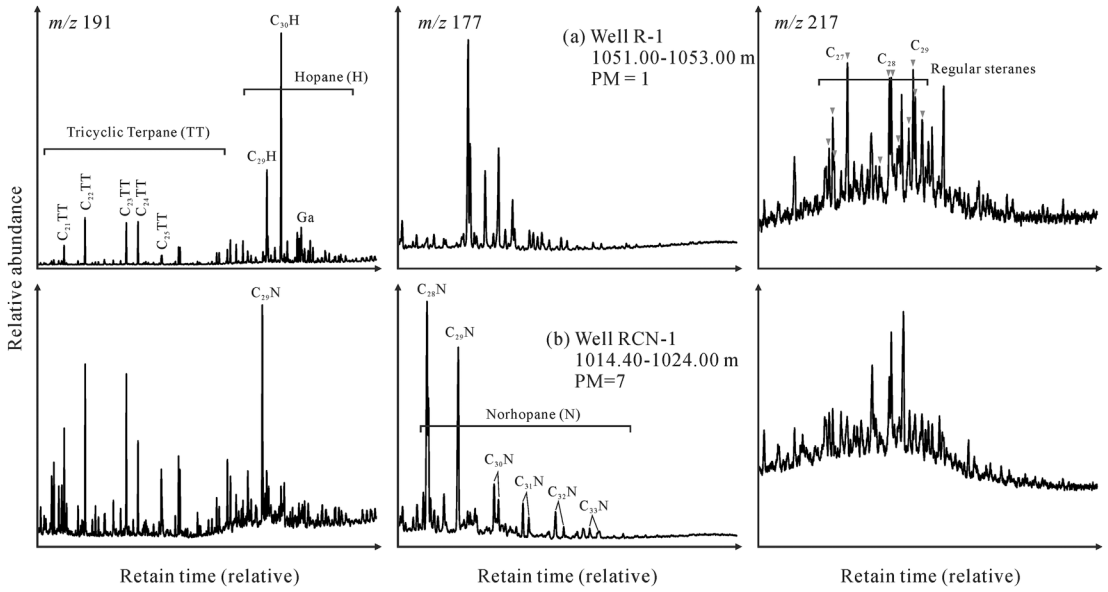

Fig. 3. Representative mass chromatograms (*m/z* 191, *m/z* 177 and *m/z* 217) of different levels of biodegradation crude oils from the Bongor Basin.

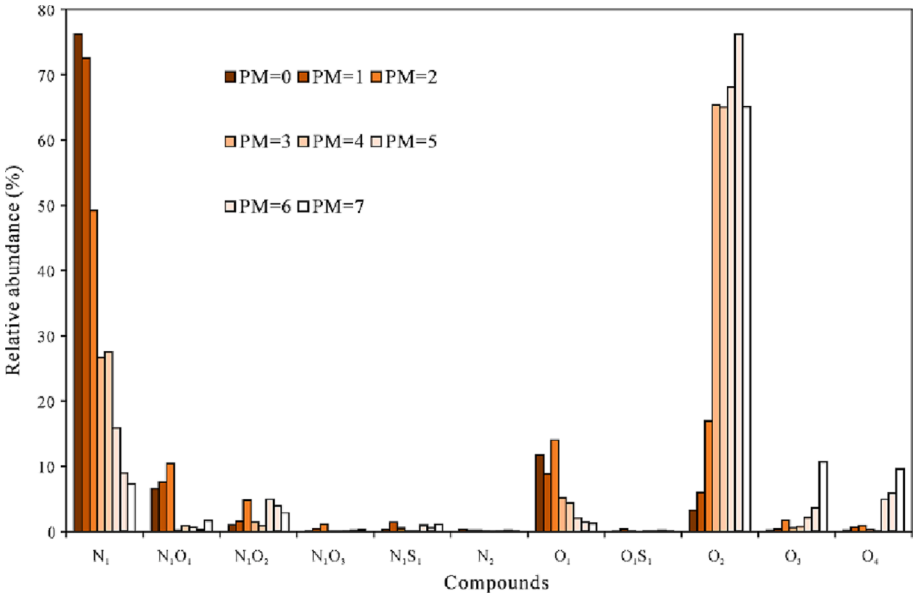

Fig. 4. The histograms showing the relative content of compound classes in different degree of biodegradation oils.

and O_1 classes decrease whereas O_2, O_3 and O_4 tend to increase with the increase of biodegradation. The high O_2 class content of the highly to strongly biodegraded oils (samples of PM = 4–7) is mostly caused by the oxidation of hydrocarbons to produce acid compounds.

4.3. Distribution of O-containing compounds

4.3.1. O_1 species

Fig. 5 shows the distribution of O_1 species in different degree of biodegradation oils. The results suggest the DBE (Double Bond Equivalent) values of O_1 species main range in 4–17. The species with a DBE of 4 may be alkylphenols rather than hydroxyl compounds [35]. The DBE values of O_1 species lightly shift to higher DBE numbers with the increasing of biodegradation. High content of DBE values of 4–7 is a characteristic of non-biodegraded oil (Fig. 5a), whereas strong biodegraded crude oil exhibits high content of DBE values of 8–13 (Fig. 5h).

4.3.2. O_2 species

Naphthenic acids are structures with acidic oxygenated functionalities with the formula $C_nH_{2n+z}O_2$, where n is referred to the number of carbon atoms and z represents the hydrogen deficiency [66]. The empirical formulas differ by CH_2 for a given hydrogen deficiency, and they differ by H_2 between z series [67]. And, a useful visualization method has been applied to categorize the data in terms of double bond equivalents (DBE) instead of empirical formulas by numerous authors, as calculated from the equation of DBE = c − h/2 + n/2 + 1 for $C_cH_hN_nO_oS_s$, which is strongly convenient to characterized highly complex samples [68–70]. Therefore, the ring number of O_2 compounds can be confirmed by the DBE values. The DBE value of fatty acids is one. It must be one more DBE for each additional ring or double bond. The O_2 species with DBE = 2 may have one ring and those with DBE = 3 may indicate two rings.

The relative content of O_2 species tends to increase with the increase of biodegradation (Fig. 6). Ethers and ketones are difficult to ionization

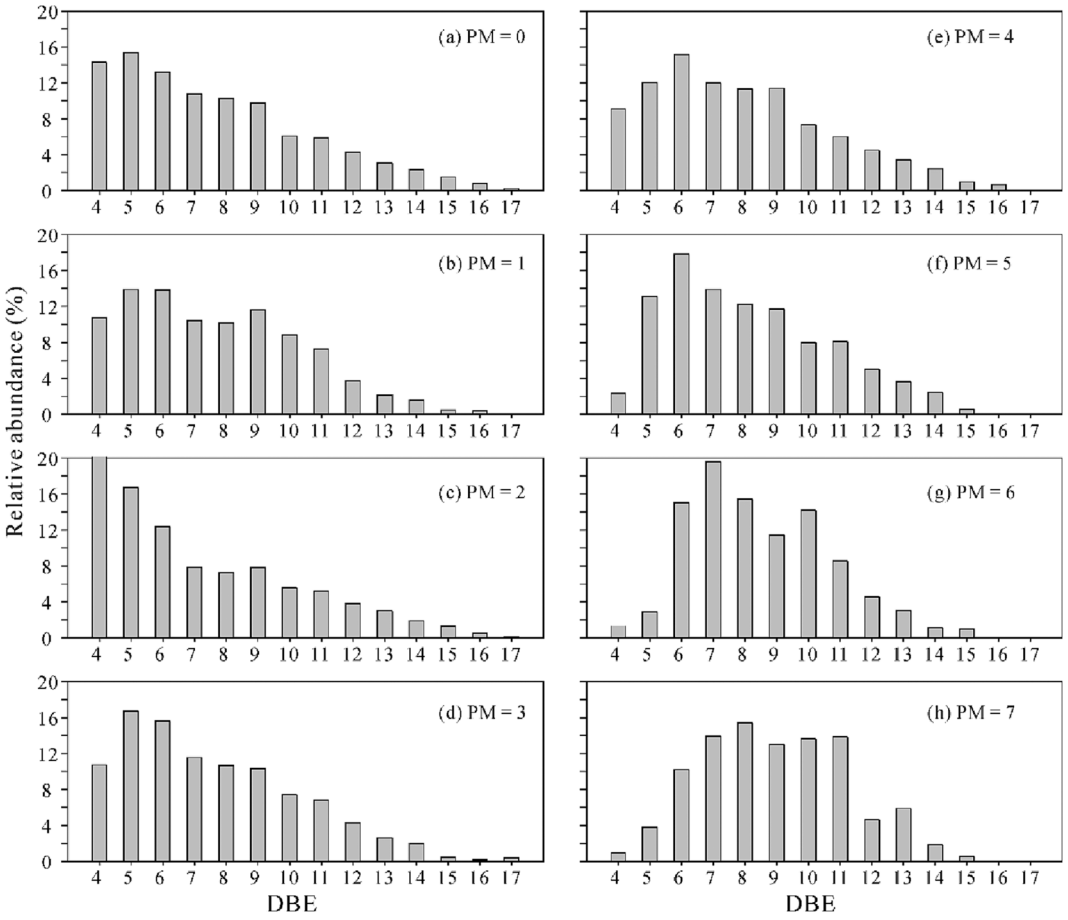

Fig. 5. Relative abundance of O_1 class in different degree of biodegradation oils.

using the negative ion ESI. O_2 species may be acids and dihydric alcohol compound. However, alcohols are easily oxidized to acids. Therefore, it could to be inferred that O_2 species are mainly acids in crude oil. In non-biodegraded oil (PM = 0), the abundance of O_2 class is much lower than those of biodegraded oil (Fig. 6a). Fatty acids (DBE = 1) occur in the light biodegraded crude oil (PM = 1 and PM = 2) (Fig. 6b, c). The fatty acids become gradually decreased relative to naphthenic acids with the increase of biodegradation. Naphthenic acids are a typical of O_2 species in high levels of biodegraded oil samples. PM = 5 sample contains a high concentration of 1-ring and 2-ring acids (Fig. 6e). In the most degraded oil (PM = 7), polycyclic acid (3-, 4-, and 5-rings) predominate (Fig. 6h). As a result, the relative abundance of naphthenic acids with high ring numbers increases as biodegradation progresses.

As shown in Fig. 10, the O_2 species is abundant in the heavily biodegraded oils (Fig. 6e-h), most likely attributable to unremitting carboxylation with the increasing of biodegradation degrees. The O_2 species with DBE = 6 is mainly referred to hopanoic acids with 5 rings. The hopanoic acids are being generated by some specific bacteria, i.e. degrading bacteria. The various changes in the distributions of hopanoic acid changes in microbial population as biodegradation proceeds [55]. C_{30}-C_{32} hopanoic acids occurred in moderately biodegraded crude oils (Fig. 6e). The contents of hopanoic acids increase with the increasing of biodegradation levels (Fig. 6h), may indicating an expansion of the bacterial community. However, the occurrence of hopanoic acids in sample with PM = 2 (Fig. 6c) may imply the different bacterial species.

4.3.3. O_3 and O_4 species

The relative abundance of O_3 and O_4 species in non-biodegraded and biodegraded oil is distinctly lower than N_1, O_1 and O_2 species. The content of O_3 and O_4 species appears to increase firstly and then decrease and finally increase with the increase of biodegradation (Fig. 4). O_3 species may be intermediate metabolites and O_4 species bear two carbonyls.

4.4. Distribution of N-containing compounds

4.4.1. N_1 Species

Both types of basic and neutral nitrogen-containing compounds occurred in crude oils [71]. The neutral nitrogen organic compounds generally comprise pyrrole, carbazole and their alkylated and benzoalkylated derivatives. The basic nitrogen forms mainly consist of pyridine, quinoline and benzoquinoline. In general, the content of the basic nitrogen compounds is much lower [72–73], while the neutral nitrogen compounds are dominant in crude oil and have been widely applied to assess maturity and predict oil filling orientation [74–80]. The neutral nitrogen compound can be analyzed using FT ICR MS in negative ion mode. N_1 species are predominant in the non-biodegraded and light biodegraded oil, and their abundance become gradually less content relative to O_2 class with the increasing of biodegradation (Fig. 4). The N_1 species are mainly composed of carbazoles (DBE = 9), benzocarbazoles (DBE = 12), dibenzocarbazoles (DBE = 15) and phenylindoles (DBE = 10) (Fig. 7). The relative abundance of N_1 species with higher DBE values, i.e. dibenzocarbazoles (DBE = 15) and benzonaphthocarbazoles (DBE = 18), tend to increase relative to carbazoles (DBE = 9) with the increasing of biodegradation. This change may be attributed to the strong anti-biodegradation of N_1 species higher DBE values and the microbial consumption of N_1 species lower DBE values.

4.4.2. N_1O_1 species

The N_1O_1 classes distributions of crude oils at different levels of

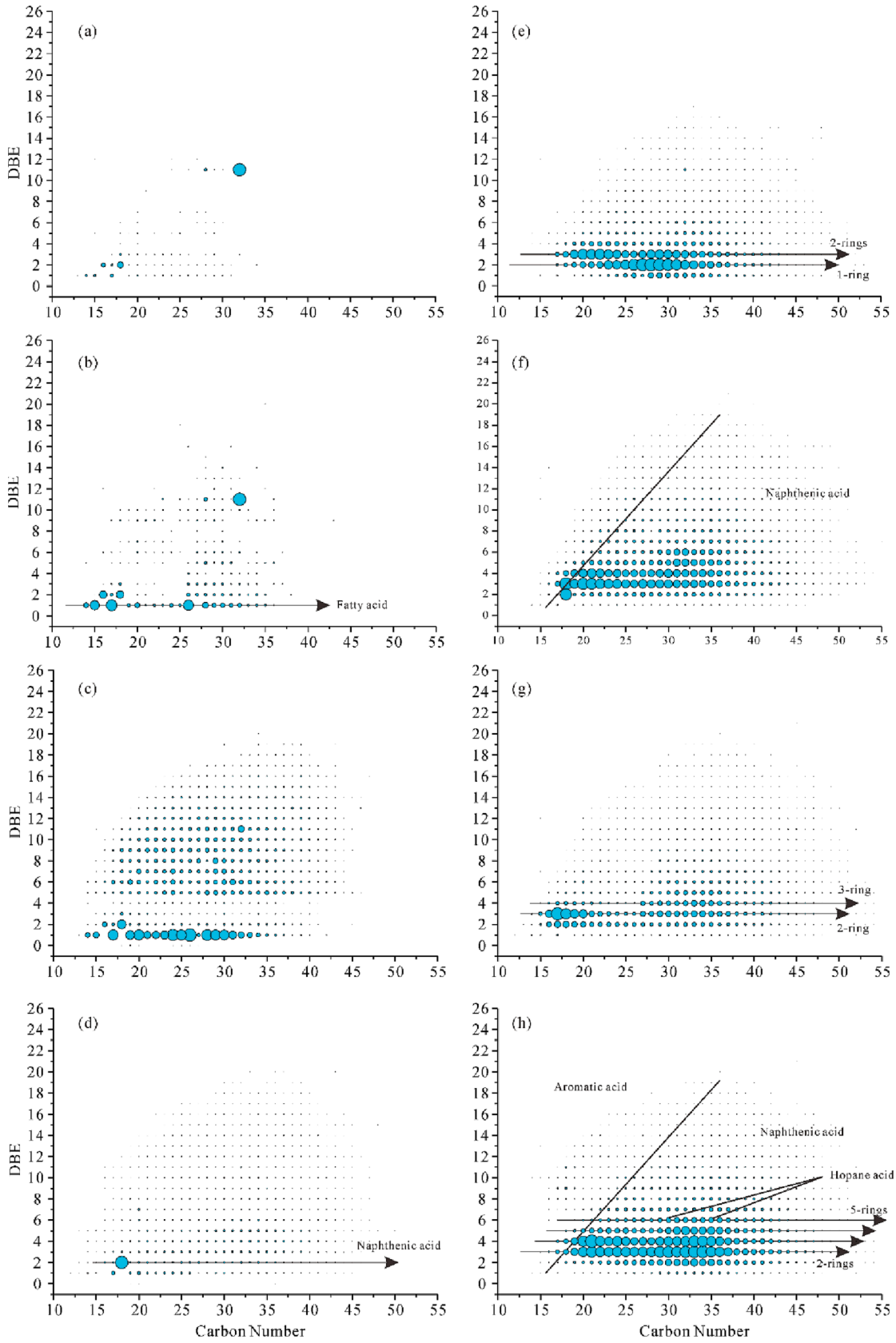

Fig. 6. Cross plots of DBE versus carbon number of the O_2 species in different degree of biodegradation oils.

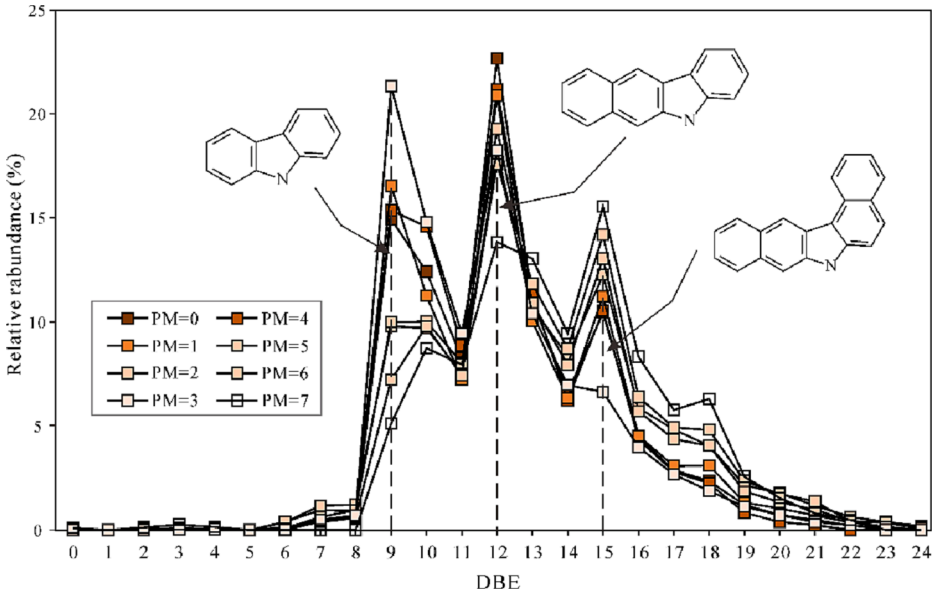

Fig. 7. Relative abundance of N_1 class in different degree of biodegradation oils.

biodegradation are illustrated in Fig. 8. The oxygen atom exhibited in N_1O_1 class may be in the form of hydroxyl. The DBE values of N_1O_1 class are ranging from 6 to 22. The N_1O_1 species are characterized by high abundance of dihydrodiol benzocarbazole (DBE = 15) and dihydrodiol dibenzocarbazoles (DBE = 18) (Fig. 8). As biodegradation proceed, the relative abundance of N_1O_x species increases when PM < 3 and then decreases when the biodegradation degree is higher than three, may indicating that N_1O_x species were the intermediate products during the biodegradation of N_1 species (Fig. 4).

5. Discussion

5.1. Biodegradation index based on O_2 species

Kim et al. (2005) observed a decrease of fatty acids and an increase of naphthenic acids with the increasing of biodegradation degree, and proposed a parameter, i.e. the ratio of acyclic to cyclic naphthenic acids (A/C ratio) based on O_2 species to define the degree of biodegradation [55]. In this study, the A/C ratio has a negative relation to the degree of biodegradation of oil samples (Fig. 9a). indicating the formation of naphthenic acids with the increase in biodegradation [47].

5.2. New parameters to determine biodegradation index

The content of S_x, S_xO_x and N_xS_x species is very lower may due to relatively low content of sulfur in selected oil samples from the Bongor Basin [63,64]. Therefore, those compounds are not considered in this study. The content of N_1 and O_1 species decreases and those of O_2, O_3 and O_4 classes increase with the increase of biodegradation show that these compounds could be considered to estimate the level of biodegradation (Fig. 4). N_1 and O_1 species are oxidized to form acids (O_2, O_3 and O_4 classes). Here, we proposed another biodegradation parameter the ratios of the sum of O_2, O_3 and O_4 species ($O_2 + O_3 + O_4$) and the sum of N_1 and O_1 species ($N_1 + O_1$). The results show that those ratios bear a positive correlation with the degree of biodegradation of crude oil (Fig. 9b). Furthermore, based on the correlation between the ratios of

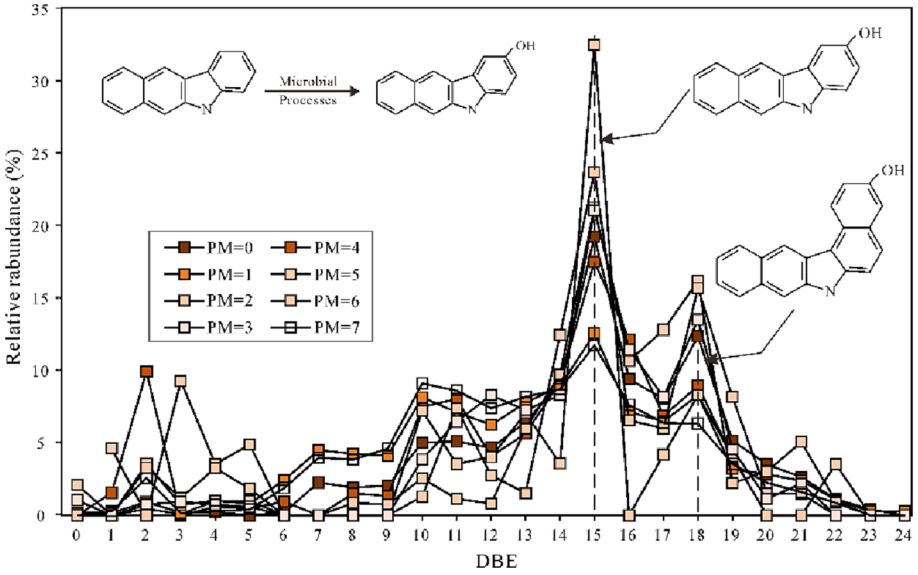

Fig. 8. Relative abundance of N_1O_1 class in different degree of biodegradation oils.

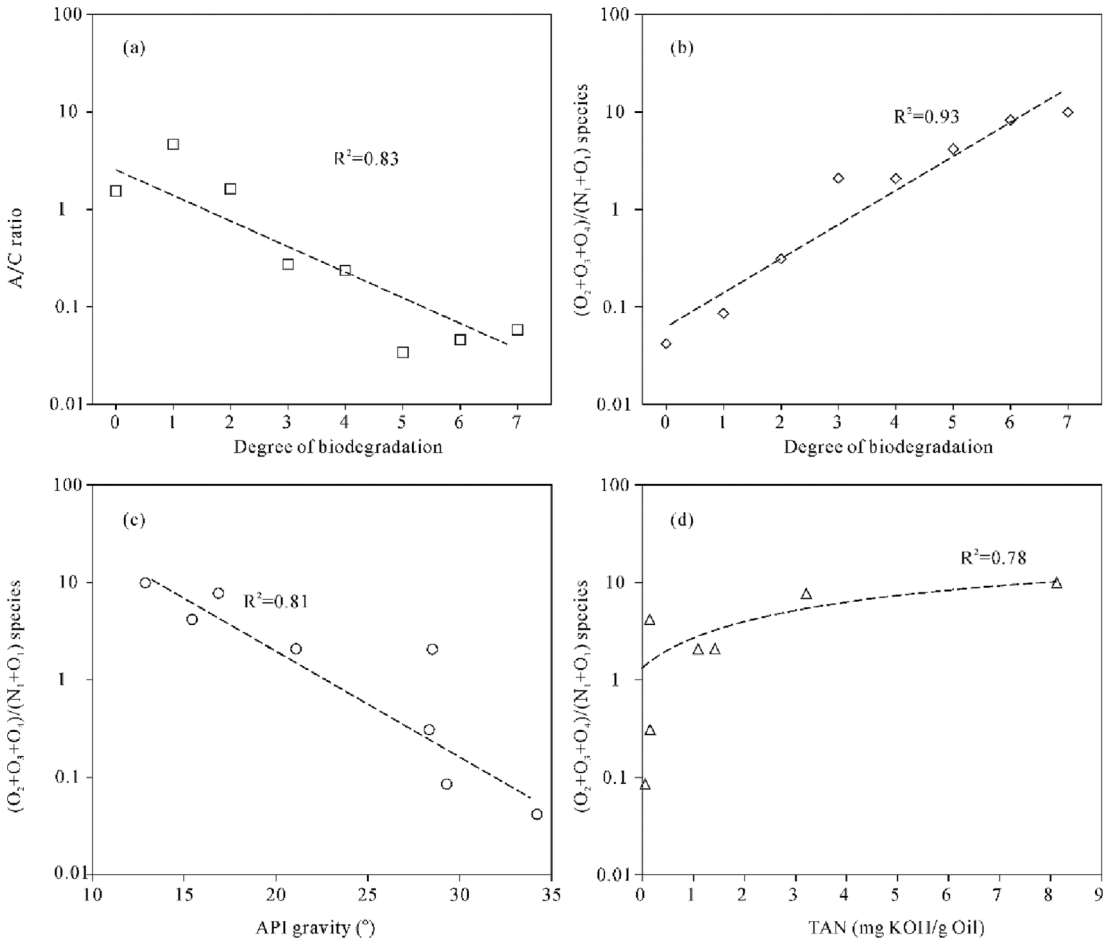

Fig. 9. Cross plot of (a) the acyclic/cyclic acid versus Biodegradation Index (modified from Kim et al. (2005) [55]); (b) the ratios of $(O_2 + O_3 + O_4)/(N_1 + O_1)$ species versus Biodegradation Index; (c) the ratios of $(O_2 + O_3 + O_4)/(N_1 + O_1)$ species versus API gravity and (d) the ratios of $(O_2 + O_3 + O_4)/(N_1 + O_1)$ species versus total acid number (TAN).

$O_2 + O_3 + O_4$ and $N_1 + O_1$ species and API gravity, this parameter could be a qualitative description of API gravity (Fig. 9c). Fig. 9 also illustrates the cross plot of total acid number (TAN) versus $(O_2 + O_3 + O_4)/(N_1 + O_1)$ species ratio in the selected crude oil samples. It shows that $(O_2 + O_3 + O_4)/(N_1 + O_1)$ species ratio bears a good correlation ($R^2 = 0.78$) with TAN in crude oils (Fig. 9d). oil. The acid fractions in non-biodegraded and lightly biodegraded oils (PM = 0–2) primarily consist of fatty acids with little in the way of naphthenic acids, leading to a low content of TAN in these oils [70]. With the increasing of biodegradation degree, the acid components are characterized by cyclic acids (e.g. mono- and dicyclic acids, hopanoid acids), resulting in a high concentration of TAN in severely biodegraded oils (PM = 4–7) [47–49].

A modified ternary diagram including N_1, O_1 and $O_2 + O_3 + O_4$ species characterized the detail changes of nitrogen- and oxygen- containing compounds (Fig. 10). Data points with high level of biodegradation tend to shift to $O_2 + O_3 + O_4$ species end-member and retreat from N_1 species end-member, showing the relative content of $O_2 + O_3 + O_4$ species increase and those of N_1 species decrease with an increasing biodegradation which may due to the formation of organic acids in degradation oil. Accordingly, the ratio of $(O_2 + O_3 + O_4)/(N_1 + O_1)$ species and new ternary diagram could be reliable tools to quantitatively estimate the biodegradation level and TAN in crude oil.

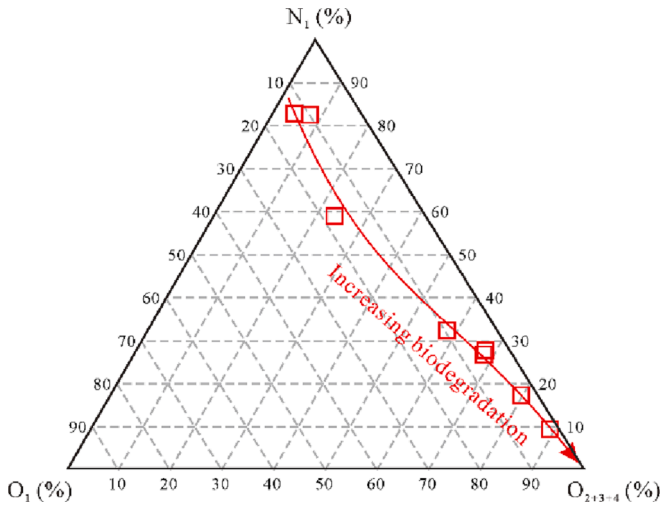

Fig. 10. Ternary diagram showing the relative abundance of N_1, O_1 and O_{2+3+4} species.

5.3. Biodegradation processes

In the initial stage of biodegradation, *n*-alkanes of saturated hydrocarbon fraction in crude oil are first consumed [8,9] (Fig. 2 a-c), and then are oxidized forming fatty acids in low grade biodegradable crude oil (Fig. 6 a-c; Fig. 9a). Next, the content of naphthenic acids in crude oil tend to increase with the increasing of biodegradation [55] (Fig. 6 d-h; Fig. 9a-b; Fig. 10). N_1- and O_1-containing compounds gradually decrease and may be convert into naphthenic acids [46,49,81,82]. N_1-containing

compounds are main compose of carbazoles, benzocarbazoles and benzonaphthocarbazoles (Fig. 7). Three biodegradation pathways of pyrrolic ring of carbazoles, i.e. ring-opening reaction, carbazole dioxygenase [55,83] (CARDO) lateral deoxygenation [84,85] and CARDO angular deoxygenation [13,84–88], have been reported. In the ring-opening reaction and CARDO angular deoxygenation of pyrrolic ring, the DBE values of N_1 class compounds would be decreased by 1 to convert into N_1O_1 and N_1O_2 species [44]. However, the DBE values of carbazoles, benzocarbazoles and benzonaphthocarbazoles would remain unchanged in CARDO lateral deoxygenation of pyrrolic ring. Based on the distribution of DBE of N_1 and N_1O_1 species (Fig. 7; Fig. 8), it shows that the degradation pathway of pyrrolic ring in N_1 class compounds includes a CARDO lateral deoxygenation that keeps DBE values in the Bongor Basin (Fig. 8).

6. Conclusions

(1) Biodegradation can influence the distribution of acids and polar NSO compounds in crude oil. The relative content of N_1, N_1O_1 and O_1 species tends to decrease and those of O_2, O_3 and O_4 species are seem to increase with the increasing of biodegradation degree.
(2) The *n*-alkanes are consumed and converted to fatty acids for the first stage of degradation and the content of naphthenic acids in crude oil tend to increase but fatty acids decrease with the increasing of biodegradation level. The most possible biodegradation pathway of carbazoles is a CARDO lateral deoxygenation to convert into N_1O_1 species compounds remain unchanged DBE values in Bongor Basin.
(3) A new biodegradation parameter, $(O_2 + O_3 + O_4)/(N_1 + O_1)$ species ratio related to acids and polar NSO compounds, is presented in this paper. This ratio indicates a good correlation with the degree of biodegradation, API gravity and TAN in crude oil, suggesting formation of acids with the increasing of biodegradation. A modified ternary diagram, including N_1, O_1, $O_2 + O_3 + O_4$ species, shows the change of compounds and biodegradation process.

CRediT authorship contribution statement

Dongyong Wang: Conceptualization, Investigation, Methodology, Formal analysis, Writing – original draft. **Meijun Li:** Conceptualization, Formal analysis, Writing – original draft, Funding acquisition. **Dingsheng Cheng:** Conceptualization, Resources. **Yebo Du:** Conceptualization, Resources. **Quan Shi:** Methodology, Supervision. **Xianli Zou:** Resources, Writing – review & editing. **Qingyao Chen:** Methodology, Investigation.

Declaration of Competing Interest

The authors declare that they have no known competing financial interests or personal relationships that could have appeared to influence the work reported in this paper.

Data availability

I have shared the link to my data/code at the Attach File step.

Acknowledgement

This work is supported by the National Natural Science Foundation of China (Grant No. 41972148). The authors thank Research Institute of Petroleum Exploration and Development, PetroChina for providing samples and permission to publish. We would like to thank the anonymous reviewers and Dr. Kevin Van Geem for their careful check and constructive comments. Thanks to Shengbao Shi, Lei Zhu and Yahe Zhang for assistance with experiments.

Appendix A. Supplementary data

Supplementary data to this article can be found online at https://doi.org/10.1016/j.fuel.2023.128438.

References

[1] Hein FJ. Geology of bitumen and heavy oil: An overview. J Pet Sci Eng 2017;154:551–63.
[2] Hein FJ. Overview of heavy oil, seeps, and oil (tar) sands. California AAPG Bull 2013;64:407–35.
[3] Hein FJ. Heavy Oil and Oil (Tar) Sands in North America: An Overview & Summary of Contributions. Nat Resour Res 2006;15:67–84.
[4] Liu W, Liao Y, Jiang C, Pan Y, Huang Y, Wang X, et al. Superimposed secondary alteration of oil reservoirs. Part II: The characteristics of biomarkers under the superimposed influences of biodegradation and thermal alteration. Fuel 2022;307:121721.
[5] Liao Y, Liu W, Pan Y, Wang X, Wang Y, Peng P. Superimposed secondary alteration of oil reservoirs. Part I: Influence of biodegradation on the gas generation behavior of crude oils. Org Geochem 2020;142:103965.
[6] Wilhelms A, Larter SR, Head I, Farrimond P, di-Primio R, Zwach C. Correction: Biodegradation of oil in uplifted basins prevented by deep burial sterilization. Nature 2001;411(6841):1034–7.
[7] Jones DM, Head IM, Gray ND, Adams JJ, Rowan AK, Aitken CM, et al. Crude-oil biodegradation via methanogenesis in subsurface petroleum reservoirs. Nature 2008;451(7175):176–80.
[8] Li Z, Huang H, Zhang S. The effect of biodegradation on bound biomarkers released from intermediate-temperature gold-tube pyrolysis of severely biodegraded Athabasca bitumen. Fuel 2020;263:116669.
[9] Huang H, Yin M, Han D. Novel parameters derived from alkylchrysenes to differentiate severe biodegradation influence on molecular compositions in crude oils. Fuel 2020;268:117366.
[10] Cheng X, Hou D, Mao R, Xu C. Severe biodegradation of polycyclic aromatic hydrocarbons in reservoired crude oils from the Miaoxi Depression. Bohai Bay Basin Fuel 2018;211:859–67.
[11] Peters KE, Moldowan JM, McCaffrey MA, Fago FJ. Selective biodegradation of extended hopanes to 25-norhopanes in petroleum reservoirs. Insights from molecular mechanics. Org Geochem 1996;24(8-9):765–83.
[12] Rowland SJ, Alexander R, Kagi RI, Jones DM. Microbial degradation of aromatic components of crude oils: A comparison of laboratory and field observations. Org Geochem 1986;9(4):153–61.
[13] Sun P, Cai C, Tang Y, Tao Z, Zhao W. A new approach to investigate effects of biodegradation on pyrrolic compounds by using a modified Manco scale. Fuel 2020;265:116937.
[14] Townsend GT, Prince RC, Suflita JM. Anaerobic biodegradation of alicyclic constituents of gasoline and natural gas condensate by bacteria from an anoxic aquifer. FEMS Microbiol Ecol 2004;49:129–35.
[15] Peters KE, Walters CC, Moldowan JM. The Biomaker Guide: Biomakers and Isotopes in Petroleum Exploration and Earth. History 2005;2:660–1.
[16] Volkman JK, Alexander R, Kagi RI, Woodhouse GW. Demethylated hopanes in crude oils and their applications in petroleum geochemistry. Geochim Cosmochim Acta 1983;47(4):785–94.
[17] Wenger LM, Davis CL, Isaksen GH. Multiple controls on petroleum biodegradation and impact on oil quality. SPE Reserv Eval Eng 2002;5:375–83.
[18] Marshall AG, Hendrickson CL, Jackson GS. Fourier transform ion cyclotron resonance mass spectrometry: a primer. Mass Spectrom Rev 1998;17(1):1–35.
[19] Hendrickson CL, Emmett MR. Electrospray ionization fourier transtorm ion cyclotron resonance mass spectrometry. Annu Rev Phys Chem 1999;50:517–36.
[20] Corilo YE, Vaz BG, Simas RC, Lopes Nascimento HD, Klitzke CF, Pereira RCL, et al. Petroleomics by EASI(±) FT-ICR MS. Anal Chem 2010;82(10):3990–6.
[21] Hertzog J, Carré V, Le Brech Y, Mackay CL, Dufour A, Mašek O, et al. Combination of electrospray ionization, atmospheric pressure photoionization and laser desorption ionization Fourier transform ion cyclotronic resonance mass spectrometry for the investigation of complex mixtures – Application to the petroleomic analysis of bio-oils. Anal Chim Acta 2017;969:26–34.
[22] Shi Q, Zhao S, Xu Z, Chung KH, Zhang Y, Xu C. Distribution of acids and neutral nitrogen compounds in a Chinese crude oil and its fractions: Characterized by negative-ion electrospray ionization fourier transform ion cyclotron resonance mass spectrometry. Energy Fuels 2010;24(7):4005–11.
[23] Vanini G, Barra TA, Souza LM, Madeira NCL, Gomes AO, Romão W, et al. Characterization of nonvolatile polar compounds from Brazilian oils by electrospray ionization with FT-ICR MS and Orbitrap-MS. Fuel 2020;282:118790.
[24] Barrow MP, McDonnell LA, Feng X, Walker J, Derrick PJ. Determination of the nature of naphthenic acids present in crude oils using nanospray Fourier transform ion cyclotron resonance mass spectrometry: The continued battle against corrosion. Anal Chem 2003;75:860–6.
[25] Han Y, Noah M, Lüders V, Horsfield B, Mangelsdorf K. NSO-compounds in oil-bearing fluid inclusions revealed by FT-ICR-MS in APPI (+) and ESI (−) modes: A new method development. Org Geochem 2020;149:104113.
[26] Han Y, Noah M, Lüders V, Körmös S, Schubert F, Poetz S, et al. Fractionation of hydrocarbons and NSO-compounds during primary oil migration revealed by high

resolution mass spectrometry: Insights from oil trapped in fluid inclusions. Int J Coal Geol 2022;254:103974.
[27] Hughey CA, Rodgers RP, Marshall AG, Qian K, Robbins WK. Identification of acidic NSO compounds in crude oils of different geochemical origins by negative ion electrospray Fourier transform ion cyclotron resonance mass spectrometry. Org Geochem 2002;33(7):743–59.
[28] Ji H, Li S, Greenwood P, Zhang H, Pang X, Xu T, et al. Geochemical characteristics and significance of heteroatom compounds in lacustrine oils of the Dongpu Depression (Bohai Bay Basin, China) by negative-ion Fourier transform ion cyclotron resonance mass spectrometry. Mar Petrol Geol 2018;97:568–91.
[29] Jiang B, Zhan Z-W, Shi Q, Liao Y, Zou Y-R, Tian Y, et al. Chemometric unmixing of petroleum mixtures by negative ion ESI FT-ICR MS analysis. Anall Chem 2019;91(3):2209–15.
[30] Oldenburg TBP, Brown M, Bennett B, Larter SR. The impact of thermal maturity level on the composition of crude oils, assessed using ultra-high resolution mass spectrometry. Org Geochem 2014;75:151–68.
[31] Poetz S, Horsfield B, Wilkes H. Maturity-driven generation and transformation of acidic compounds in the organic-rich Posidonia Shale as revealed by electrospray ionization Fourier transform ion cyclotron resonance mass spectrometry. Energy Fuels 2014;28(8):4877–88.
[32] Wan Z, Li S, Pang X, Dong Y, Wang Z, Chen X, et al. Characteristics and geochemical significance of heteroatom compounds in terrestrial oils by negative-ion electrospray Fourier transform ion cyclotron resonance mass spectrometry. Org Geochem 2017;111:34–55.
[33] Wang Qi, Hao F, Cao Z, Tian J. Heteroatom compounds in oils from the Shuntuoguole low uplift, Tarim Basin characterized by (+ESI) FT-ICR MS: Implications for ultra-deep petroleum charges and alteration. Mar Petrol Geol 2021;134:105321.
[34] Yan G, Xu Y, Liu Y, He W, Chang X, Tang P. The evolution of acids and neutral nitrogen-containing compounds during pyrolysis experiments on immature mudstone. Mar Petrol Geol 2020;115:104292.
[35] Ziegs V, Noah M, Poetz S, Horsfield B, Hartwig A, Rinna J, et al. Unravelling maturity- and migration-related carbazole and phenol distributions in Central Graben crude oils. Mar Petrol Geol 2018;94:114–30.
[36] Zhang H, Li S. GC–MS and ESI FT-ICR MS characterization on two type crude oils from the Dongying depression. Fuel 2023;333:126408.
[37] Han Y, Poetz S, Mahlstedt N, Karger C, Horsfield B. Fractionation and origin of NyOx and Ox compounds in the Barnett Shale sequence of the Marathon 1 Mesquite well. Texas Mar Petrol Geol 2018;97:517–24.
[38] Liu P, Li M, Jiang Q, Cao T, Sun Y. Effect of secondary oil migration distance on composition of acidic NSO compounds in crude oils determined by negative-ion electrospray Fourier transform ion cyclotron resonance mass spectrometry. Org Geochem 2015;78:23–31.
[39] de Aguiar DVA, da Silva Lima G, da Silva RR, Júnior IM, Gomes AdO, Mendes LAN, et al. Comprehensive composition and comparison of acidic nitrogen- and oxygen-containing compounds from pre- and post-salt Brazilian crude oil samples by ESI (-) FT-ICR MS. Fuel 2022;326:125129.
[40] Meng Q, Wang X, Liao Y, Lei Y, Yin J, Liu P, et al. The effect of slight to moderate biodegradation on the shale soluble organic matter composition of the upper triassic Yanchang formation, Ordos Basin. China Mar Petrol Geol 2021;128:105021.
[41] Santos J, Wisniewski Jr A, Eberlin M, Schrader W. Comparing crude oils with different API gravities on a molecular level using mass spectrometric analysis. Part 1: Whole Crude Oil. Energies 2018;11:2766.
[42] Liu W, Liao Y, Pan Y, Jiang B, Zeng Q, Shi Q, et al. Use of ESI FT–ICR MS to investigate molecular transformation in simulated aerobic biodegradation of a sulfur-rich crude oil. Org Geochem 2018;123:17–26.
[43] Oldenburg TBP, Jones M, Huang H, Bennett B, Shafiee NS, Head I, et al. The controls on the composition of biodegraded oils in the deep subsurface – Part 4. Destruction and production of high molecular weight non-hydrocarbon species and destruction of aromatic hydrocarbons during progressive in-reservoir biodegradation. Org Geochem 2017;114:57–80.
[44] Pan Y, Liao Y, Shi Q, Hsu CS. Acidic and neutral polar NSO compounds in heavily biodegraded oils characterized by negative-ion ESI FT-ICR MS. Energy Fuels 2013;27(6):2960–73.
[45] Yang BaiBing, Xu ChunMing, Zhao SuoQi, Hsu CS, Chung KH, Shi Q. Thermal transformation of acid compounds in high TAN crude oil. Sci China Chem 2013;56(7):848–55.
[46] Hughey CA, Galasso SA, Zumberge JE. Detailed compositional comparison of acidic NSO compounds in biodegraded reservoir and surface crude oils by negative ion electrospray Fourier transform ion cyclotron resonance mass spectrometry. Fuel 2007;86(5-6):758–68.
[47] Li M, Cheng D, Pan X, Dou L, Hou D, Shi Q, et al. Characterization of petroleum acids using combined FT-IR, FT-ICR–MS and GC–MS: Implications for the origin of high acidity oils in the Muglad Basin. Sudan Org Geochem 2010;41(9):959–65.
[48] Mapolelo MM, Rodgers RP, Blakney GT, Yen AT, Asomaning S, Marshall AG. Characterization of naphthenic acids in crude oils and naphthenates by electrospray ionization FT-ICR mass spectrometry. Int J Mass Spectrom 2011;300(2-3):149–57.
[49] Barros EV, Filgueiras PR, Lacerda V, Rodgers RP, Romão W. Characterization of naphthenic acids in crude oil samples – A literature review. Fuel 2022;319:123775.
[50] Ni W, Zhu G, Liu F, Xie C, Li W, Zhu S. Rapid profiling of carboxylic acids in reservoir biodegraded crude oils using gas purge microsyringe extraction coupled to comprehensive two-dimensional gas chromatography-mass spectrometry. Fuel 2022;316:123312.
[51] Cheng D, Dou L, Xiao K, Wan K, Liu B. Origin of high acidity oils in the intensively inversed rift basin. Bongor Basin Acta Petrol Sinica 2014;30:789–800.
[52] Cheng, D., Dou, L., Shi, B., Ma, L., Xiao, K., Li, Z. Origin of high acidity oils in the Palogue Oilfield, Melut Basin, Sudan. Pet Explor Dev 2010;37:568-72+622.
[53] Cheng D, Dou L, Wan K, Shi Q. Formation mechanism analysis of Sudan high acidity oils by electrospray ionization fourier transform ion cyclotron resonance mass spectrometry. Acta Petrol Sinica 2010;26:1303–12.
[54] Cheng D, Dou L, Li Y, Li Z. Component and distribution of organic acid oil with high TAN, M Basin, Sudan. Pet Explor Dev 2006:762–5.
[55] Kim S, Stanford LA, Rodgers RP, Marshall AG, Walters CC, Qian K, et al. Microbial alteration of the acidic and neutral polar NSO compounds revealed by Fourier transform ion cyclotron resonance mass spectrometry. Org Geochem 2005;36(8):1117–34.
[56] Genik GJ. Petroleum Geology of Cretaceous-Tertiary rift basins in Niger, Chad, and Central African Republic. AAPG Bull 1993;77:1405–34.
[57] Guiraud R, Binks RM, Fairhead JD, Wilson M, Ziegler PA. Chronology and geodynamic setting of Cretaceous-Cenozoic rifting in West and Central Africa. Tectonophysics 1992;213:227–34.
[58] Dou L, Wang J, Wang R, Wei X, Shrivastava C. Precambrian basement reservoirs: Case study from the northern Bongor Basin, the Republic of Chad. AAPG Bull 2018;102(09):1803–24.
[59] Dou L, Cheng D, Du Y, Xiao G, Wang J, Wang R. Petroleum systems of the Bongor Basin and the great Baobad oilfield. Southern Chad J Petrol Geol 2022;43:301–22.
[60] Dou L, Li W, Cheng D. Hydrocarbon accumulation period and process in Baobab area of Bongor Basin. J African Earth Sci 2020;161:103673.
[61] Chen L, Ji H, Dou L, Du Y, Xu Z, Zhang L, et al. The characteristics of source rock and hydrocarbon charging time of Precambrian granite reservoirs in the Bongor Basin. Chad Mar Petrol Geol 2018;97:323–38.
[62] Yang X, Ji H, Dou L, Du Y, Jia H, Chen L, et al. Tectono-sedimentary characteristics in the area with distributed normal faults: Lower Cretaceous Prosopis Formation in the northern slope of Bongor Basin. Chad J Pet Sci Eng 2020;190:107081.
[63] Cheng D, Dou L, Chen Q, Wang W. Geochemical characteristics and origins of biodegraded oils in the Bongor Basin (Chad) and their implications for petroleum exploration. Energy Explor Exploit 2022;40(2):682–700.
[64] Song H, Wen Z, Bao J. Influence of biodegradation on carbazole and benzocarbazole distributions in oils from the Bongor Basin. Chad Org Geochem 2016;100:18–28.
[65] Li N, Huang H, Jiang W, Wu T, Sun J. Biodegradation of 25-norhopanes in a Liaohe Basin (NE China) oil reservoir. Org Geochem 2015;78:33–43.
[66] Dzidic I, Somerville AC, Raia JC, Hart HV. Determination of naphthenic acids in California crudes and refinery wastewaters by fluoride ion chemical ionization mass spectrometry. Anal Chem 1988;60(13):1318–23.
[67] Hsu CS, Dechert GJ, Robbins WK, Fukuda EK. Naphthenic acids in crude oils characterized by mass spectrometry. Energy Fuels 2000;14(1):217–23.
[68] Fu J, Klein GC, Smith DF, Kim S, Rodgers RP, Hendrickson CL, et al. Comprehensive compositional analysis of hydrotreated and untreated nitrogen-concentrated fractions from syncrude oil by electron ionization, field desorption ionization, and electrospray ionization ultrahigh-resolution FT-ICR mass spectrometry. Energy Fuels 2006;20(3):1235–41.
[69] Panda SK, Andersson JT, Schrader W. Mass-spectrometric analysis of complex volatile and nonvolatile crude oil components: a challenge. Anal Bioanal Chem 2007;389(5):1329–39.
[70] Barrow MP, Headley JV, Peru KM, Derrick PJ. Data visualization for the characterization of naphthenic acids within petroleum samples. Energy Fuels 2009;23(5):2592–9.
[71] Richter FP, Caesar PD, Meisel SL, Offenhauer RD. Distribution of nitrogen in petroleum according to basicity. Ind Eng Chem 1952;44(11):2601–5.
[72] Li M, Larter SR. Potential bias in the isolation of pyridinic nitrogen fractions from crude oils and rock extracts using acid extraction and liquid chromatography. Org Geochem 2001;32(8):1025–30.
[73] Prado GHC, Rao Y, de Klerk A. Nitrogen removal from oil: a review. Energy Fuels 2017;31(1):14–36.
[74] Carvalho Dias L, Bomfim Bahia PV, Nery do Amaral D, Machado ME. Nitrogen compounds as molecular markers: An overview of analytical methodologies for its determination in crude oils and source rock extracts. Microchem J 2020;157:105039.
[75] Li M, Yao H, Stasiuk LD, Fowler MG, Larter SR. Effect of maturity and petroleum expulsion on pyrrolic nitrogen compound yields and distributions in Duvernay Formation petroleum source rocks in central Alberta. Canada Org Geochem 1997;26(11-12):731–44.
[76] Bennett B, Olsen SD. The influence of source depositional conditions on the hydrocarbon and nitrogen compounds in petroleum from central Montana, USA. Org Geochem 2007;38(6):935–56.
[77] Clegg H, Wilkes H, Horsfield B. Carbazole distributions in carbonate and clastic source rocks. Geochim Cosmochim Acta 1997;61(24):5335–45.
[78] Larter SR, Bowler BFJ, Li M, Chen M, Brincat D, Bennett B, et al. Molecular indicators of secondary oil migration distances. Nature 1996;383(6601):593–7.
[79] Han Q, Li M, Liu X, Jiang W, Shi S, Tang Y, et al. Fractionation of alkylated carbazoles in petroleum during subsurface migration: Evidence from molecular simulation and application in sandstone reservoirs. J Pet Sci Eng 2020;191:107308.
[80] Terra LA, Filgueiras PR, Tose LV, Romão W, de Castro EVR, de Oliveira LMSL, et al. Laser desorption ionization FT-ICR mass spectrometry and CARSPLS for predicting basic nitrogen and aromatics contents in crude oils. Fuel 2015;160:274–81.

[81] Tomczyk NA, Winans RE, Shinn JH, Robinson RC. On the nature and origin of acidic species in petroleum. 1. Detailed acid type distribution in a California crude oil. Energy Fuels 2001;15(6):1498–504.
[82] Aitken CM, Jones DM, Larter SR. Anaerobic hydrocarbon biodegradation in deep subsurface oil reservoirs. Nature 2004;431(7006):291–4.
[83] Liao Y, Shi Q, Hsu CS, Pan Y, Zhang Y. Distribution of acids and nitrogen-containing compounds in biodegraded oils of the Liaohe Basin by negative ion ESI FT-ICR MS. Org Geochem 2012;47:51–65.
[84] Nojiri H, Nam J-W, Kosaka M, Morii K-I, Takemura T, Furihata K, et al. Diverse oxygenations catalyzed by carbazole 1,9a-dioxygenase from Pseudomonas sp. Strain CA10. J Bacteriol 1999;181(10):3105–13.
[85] Takagi T, Nojiri H, Yoshida T, Habe H, Omori T. Detailed comparison between the substrate specificities of two angular dioxygenases, dibenzofuran 4,4a-dioxygenase from Terrabacter sp. and carbazole 1,9a-dioxygenase from Pseudomonas resinovorans. Biotechno Lett 2002;24:2099–106.
[86] Ouchiyama N, Zhang Y, Omori T, Kodama T. Biodegradation of Carbazole by Pseudomonas spp. CA06 and CA10. Biosci Biotech Bioch 1993;57(3):455–60.
[87] Sato SI, Nam JW, Kasuga K, Nojiri H, Yamane H, Omori T. Identification and characterization of genes encoding carbazole 1,9a-dioxygenase in Pseudomonas sp. strain CA10. J Bacteriol 1997;179(15):4850–8.
[88] Sato SI, Ouchiyama N, Kimura T, Nojiri H, Yamane H, Omori T. Cloning of genes involved in carbazole degradation of Pseudomonas sp. strain CA10: nucleotide sequences of genes and characterization of meta-cleavage enzymes and hydrolase. J Bacteriol 1997;179(15):4841–9.